PDK2-mediated alternative splicing switches Bnip3 from cell death to cell survival

Hongying Gang,[1,2] Rimpy Dhingra,[1,2] Junjun Lin,[1,2] Yan Hai,[1,2] Yaron Aviv,[1,2] Victoria Margulets,[1,2] Mohammad Hamedani,[3] Thatchawan Thanasupawat,[5] Etienne Leygue,[3] Thomas Klonisch,[5] James R. Davie,[4] and Lorrie A. Kirshenbaum[1,2]

[1]Department of Physiology, The Institute of Cardiovascular Sciences, St. Boniface Hospital Research Centre, [2]Department of Pathophysiology, The Institute of Cardiovascular Sciences, St. Boniface Hospital Research Centre, [3]Department of Biochemistry and Medical Genetics, [4]Manitoba Institute for Child Health, and [5]Department of Anatomy and Cell Science, College of Medicine, Faculty of Health Sciences, University of Manitoba, Winnipeg, Manitoba, R2H 2A6

Herein we describe a novel survival pathway that operationally links alternative pre-mRNA splicing of the hypoxia-inducible death protein Bcl-2 19-kD interacting protein 3 (Bnip3) to the unique glycolytic phenotype in cancer cells. While a full-length Bnip3 protein (Bnip3FL) encoded by exons 1–6 was expressed as an isoform in normal cells and promoted cell death, a truncated spliced variant of Bnip3 mRNA deleted for exon 3 (Bnip3Δex3) was preferentially expressed in several human adenocarcinomas and promoted survival. Reciprocal inhibition of the Bnip3Δex3/Bnip3FL isoform ratio by inhibiting pyruvate dehydrogenase kinase isoform 2 (PDK2) in Panc-1 cells rapidly induced mitochondrial perturbations and cell death. The findings of the present study reveal a novel survival pathway that functionally couples the unique glycolytic phenotype in cancer cells to hypoxia resistance via a PDK2-dependent mechanism that switches Bnip3 from cell death to survival. Discovery of the survival Bnip3Δex3 isoform may fundamentally explain how certain cells resist Bnip3 and avert death during hypoxia.

Introduction

Genetically unstable or damaged cells are discarded by the body by programmed apoptosis or necrosis, respectively. Defects in the regulatory processes that govern cell death have been linked to a variety of human pathologies including neurodegenerative diseases and cancer (Ashwell et al., 1994). Indeed, the ability of cancer cells to circumvent death during hypoxia or nutrient stress is a well-established and acknowledged feature of tumorigenesis (Gatenby et al., 2007; Chiche et al., 2010). The prevailing mechanism by which cancers avert cell death under low oxygen tension is poorly understood but has been suggested to involve adaptive reprogramming of genes associated with cell survival and metabolism (Plas and Thompson, 2002). Because early carcinogenesis typically occurs in a hypoxic microenvironment, the tumor cells rely on glycolysis for energy production (Gatenby et al., 2007; Gillies and Gatenby, 2007a; Robey et al., 2008). Therefore, even though the tumors eventually become vascularized and O_2 levels increase, the glycolytic phenotype persists, resulting in the "paradox" of glycolysis during aerobic conditions (the Warburg effect; Warburg, 1956; Robey et al., 2008). This property of cancerous and hypoxic tumors has been attributed in part to the enhanced expression levels of the glycolytic enzymes, notably pyruvate dehydrogenase (PDH) kinase (PDK), which inhibits the PDH. PDH is a critical mitochondrial enzyme that regulates glucose oxidation through its conversion of pyruvate to acetyl-CoA and mitochondrial pyruvate flux. Inhibition of PDH resulted in the incomplete oxidation of glucose resulting in conversion of pyruvate to lactate in cytoplasm (Gang et al., 2014). Interestingly, inhibition of the PDK isoform 2 (PDK2) with dichloroacetic acid (DCA) in certain cancer cells restored mitochondrial glucose oxidation, and sensitized cancer cells to apoptotic stimuli by activating PDH activity (Bonnet et al., 2007; Garon et al., 2014; Wojtkowiak et al., 2015). These findings support the notion that glucose metabolism in cancer cells is mutually dependent and obligatorily linked to cell survival (Gatenby and Gillies, 2007; Gillies and Gatenby, 2007b). Though an operational link between glucose utilization and hypoxia resistance has been suggested, the underlying mechanisms remain unknown (Israelsen et al., 2013).

Alternative gene splicing provides a means by which cells generate proteins with different properties from a single mRNA precursor. Indeed, alternative splicing of several metabolic and survival genes have been reported in a variety of human cancers (Christofk et al., 2008; Israelsen et al., 2013). Recent data by our laboratory established the hypoxia-inducible protein Bcl-2 19 kD interacting protein (Bnip3) to be crucial for provoking cell death of cardiac myocytes during hypoxia in vivo and in

Correspondence to Lorrie A. Kirshenbaum: Lorrie@sbrc.ca

Abbreviations used in this paper: Bnip3, Bcl-2 19-kD interacting protein 3; DCA, dichloroacetic acid; PDH, pyruvate dehydrogenase; PDK, PDH kinase; ROS, reactive oxygen species.

The Rockefeller University Press $30.00
J. Cell Biol. Vol. 210 No. 7 1101–1115
www.jcb.org/cgi/doi/10.1083/jcb.201504047

vitro (Regula et al., 2002; Dhingra et al., 2014). Importantly, we demonstrated that Bnip3 provoked mitochondrial perturbations including permeability transition pore opening, loss of mitochondrial ΔΨm, reactive oxygen species (ROS), and cell death. Furthermore, genetic ablation or mutations that abrogated mitochondrial targeting of Bnip3 suppressed mitochondrial perturbations and cell death. Collectively, these findings substantiate the importance of Bnip3 as central regulator of mitochondrial function and cell death of ventricular myocytes during hypoxic injury of postnatal ventricular myocytes. Another salient feature of Bnip3 is its reported ability to serve as a sensor of mitochondrial quality control through autophagy/mitophagy (Hamacher-Brady et al., 2006; Wang et al., 2013). Indeed, the ability of Bnip3 to be involved in some aspects of mitochondrial clearance has been reported, but this property of Bnip3 is less well understood and may be cell and context specific. Nevertheless, despite these findings substantiating Bnip3 as a critical regulator of mitochondrial injury and cell death during hypoxia, certain cancer cells are reportedly resistant to Bnip3-induced cell death (Bellot et al., 2009; Mazure and Pouysségur, 2009). The underlying mechanism that accounts for these apparent differences in the actions of Bnip3 on cell death is unknown but likely reflects an adaptive mechanism that allows tumor cells to suppress the otherwise lethal actions of Bnip3. Collectively, we believe these confounding results may be attributed to a cellular factor that antagonizes the otherwise lethal actions of Bnip3 in cancer cells.

Little is known of the mechanisms that regulate Bnip3 transcription or posttranscriptional processing under basal or apoptotic conditions. During the course of our investigations, we identified a novel previously unrecognized alternatively spliced variant of Bnip3 mRNA in cardiac muscle generated exclusively during hypoxia (Gang et al., 2011). Sequence analysis revealed that the canonical Bnip3 protein encoded by Bnip3 mRNA composed of exons 1–6, designated Bnip3FL, contains the BH3-like domain and carboxyl–terminal transmembrane (TM) required for mitochondrial membrane targeting; and that the splice variant of Bnip3 mRNA generated by exclusion of exon 3 encodes a truncated Bnip3 protein designated Bnip3Δex3, which lacked the BH3-like domain and the critical TM domain, was virtually absent in normal cells but highly expressed in several human adenocarcinomas. Interestingly, while Bnip3FL provoked widespread cell death, Bnip3Δex3 promoted survival in cardiac myocytes (Gang et al., 2011). The functional significance of the Bnip3Δex3 spliced isoform in cancer cells is unknown and has not been formally tested. Given the inherent resistant of tumor cells to tissue hypoxia, we reasoned that alternative spliced form of Bnip3Δex3 may confer an adaptive survival advantage that is linked to their unique glycolytic phenotype (Christofk et al., 2008).

In this study, we test this possibility and provide compelling new evidence that Bnip3Δex3 variant is preferentially expressed in several different human cancers where it antagonizes the actions of Bnip3FL. We further show Bnip3Δex3 mRNA synthesis is dependent on the unique glycolytic phenotype in cancer cells. Hence, the findings of the present study reveal an adaptive survival pathway for hypoxia resistance in cancer cells that is obligatorily linked and mutually dependent on the alternative splicing that switches Bnip3 from cell death to survival. The preferential synthesis of the survival isoform Bnip3Δex3 may explain more fundamentally how certain tumor cells override cell death during hypoxia.

Results

Glycolytic metabolism associated with the alternative splicing of Bnip3 in cancer cells

To begin to understand the biological significance of Bnip3Δex3 isoform in cancer cells, we formally assessed the relative expression levels of the Bnip3FL and Bnip3Δex3 isoforms in several different human cancer cell lines. For these studies, we compared the expression levels of the Bnip3 mRNA isoforms in Panc-1, HCT116, and MCF-7 cancer cells to primary cultured postnatal cardiac myocytes. Interestingly, while low levels of Bnip3FL mRNA were detectable in cardiac myocytes under basal conditions, it was virtually absent in Panc-1, HCT116, and MCF-7 cells, respectively (Fig. 1 A). Conversely, the Bnip3Δex3 isoform was highly expressed in each of the cancer cell lines tested compared with cardiac myocytes under basal conditions, with the highest level of Bnip3Δex3 expression observed in Panc-1 cells (Fig. 1 A). Further we detected the Bnip3Δex3 isoform in several different human breast tumors and glioblastomas (Fig. S1, A and B). Collectively these findings verify that Bnip3Δex3 is constitutively present as the major Bnip3 isoform in human cancers.

Because we previously demonstrated that the spliced variant Bnip3Δex3 was generated preferentially under hypoxic conditions in postnatal cardiac myocytes, we reasoned that the unique metabolic profile of cancer cells (aerobic glycolysis) might provide the glycolytic environment to favor the splicing and generation of Bnip3Δex3 isoform. To test this possibility, we assessed whether PDK2 expression, the key glycolytic enzyme that regulates mitochondria pyruvate flux, is altered in postnatal cardiac myocytes and Panc-1 cancer cells. As shown in Fig. 1 B, in contrast to cardiac myocytes that exhibited low basal levels of PDK2, PDK2 was highly expressed in Panc-1 cells, consistent with the higher levels of Bnip3Δex3 isoform observed in these cells (Fig. 1 A). Interestingly, however, PDK2 expression was markedly increased in cardiac myocytes subjected to hypoxia, coincident with an increase in Bnip3Δex3 splicing. Further, overexpression of PDK2 in cardiac myocytes under normoxic conditions recapitulated the effects of hypoxia and shifted splicing toward the Bnip3Δex3 isoform (Fig. 1 C). To determine whether the high basal levels of PDK2 in cancer cells provides the metabolic switch that favors generation of Bnip3Δex3 isoform, we monitored Bnip3 mRNA splicing by real-time PCR in Panc-1 cells in the absence or presence of the PDK2 inhibitor DCA. To first prove that PKD2 activity is inhibited by DCA in cancer cells, we assessed PDK2 protein expression and kinase activity in Panc-1 cells treated with DCA. As shown by Western blotting (Fig. 1 D), PDK2 protein expression in cells treated with DCA was not appreciably different from control; however, PKD2 kinase activity was markedly inhibited in cells treated with DCA or after PDK2 knockdown (Fig. 1 E). These findings verify that PDK2 kinase activity is indeed inhibited by DCA. Notably, inhibition of PDK2 activity in cells treated with DCA resulted in a dose-dependent reduction in Bnip3Δex3 splicing (Fig. 1 F). Because the direction of pyruvate flux controlled by the PDK–PDH pathway determines whether glucose oxidation via mitochondrial TCA will be complete or incomplete via cytoplasmic glycolysis, we reasoned that splicing of Bnip3Δex3 may be directly affected by pyruvate levels within cancer cells that exhibit high basal levels of PDK2. To test this possibility, we assessed whether altering cellular pyruvate levels would influence Bnip3Δex3

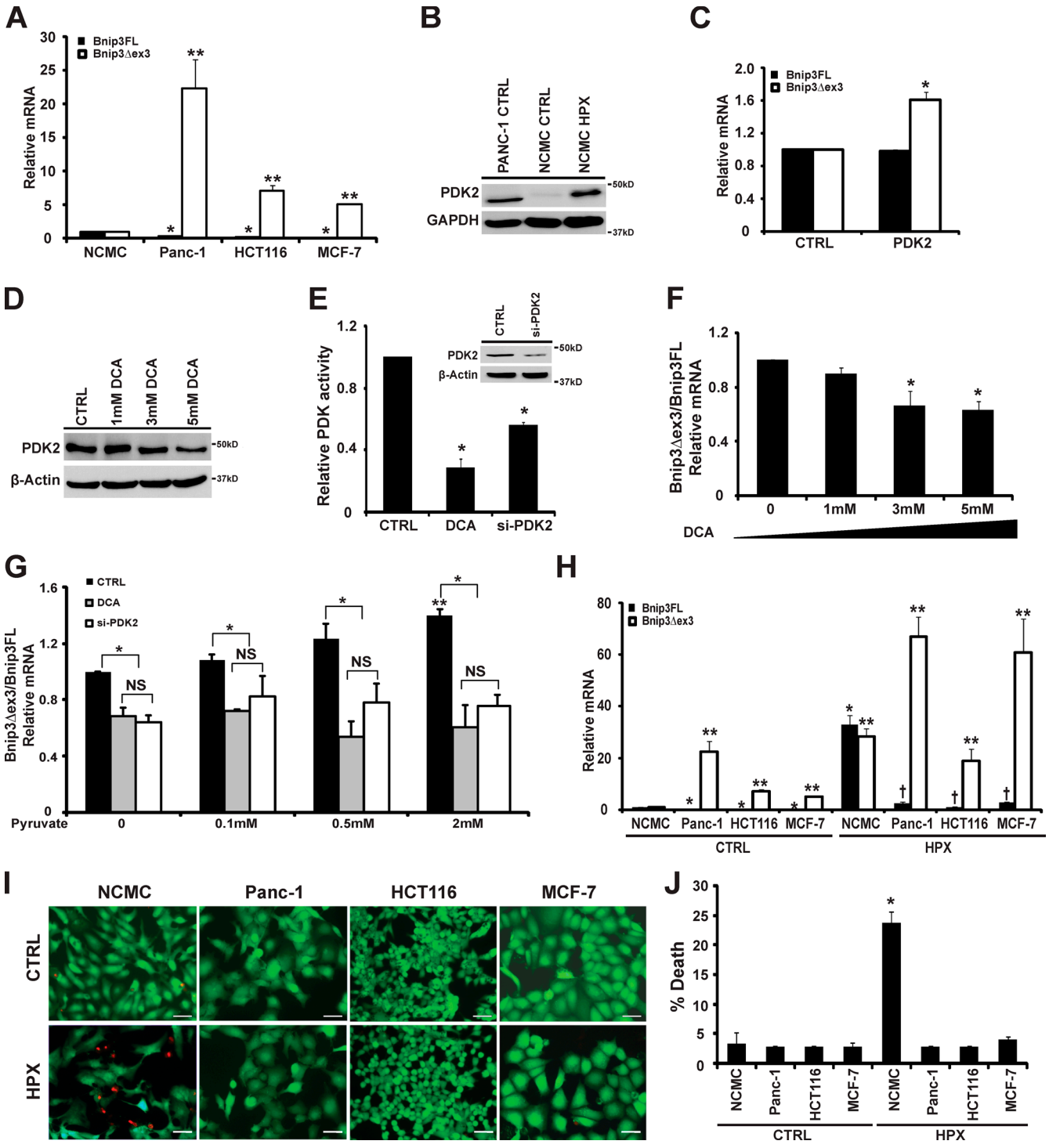

Figure 1. **Alternative splicing of Bnip3 in cancer cells.** (A) Endogenous mRNA levels of Bnip3 full length (Bnip3FL) and Bnip3 spliced variant deleted for exon 3 (Bnip3Δex3) by qPCR in neonatal cardiac myocytes (NCMC), Panc-1, HCT-116, and MCF-7 cells. Data were obtained from at least $n = 4–7$ independent experiments for each condition tested. Data are expessed as mean ± SD (error bars). *, statistically different from Bnip3FL of primary NCMC; **, statistically different from Bnip3Δex3 of NCMC. (B) Western blot analysis of endogenous PDK2 proteins in Panc-1 cells and NCMC under normoxia and hypoxia conditions. The filter was probed with an antibody directed against PDK2 (46 kD). GAPDH served as a loading control for the Western blot. (C) Endogenous mRNA expression levels of Bnip3FL and Bnip3Δex3 isoforms in NCMC transfected with vector alone control (CTRL) or PDK2 eukaryotic expression plasmid. Data were obtained from at least $n = 3$ independent experiments for each condition tested. *, statistically different from CTRL. (D) Western blot analysis of endogenous PDK2 protein in Panc-1 cells treated with 1–5 mM DCA. The filter was probed with an antibody directed against PDK2 (46 kD). β-Actin served as a loading control for the Western blot. (E) ELISA for PDK2 kinase activity in Panc-1 cells treated with 5 mM DCA or knocked down for PDK2. Data were obtained from at least $n = 4$ independent cell culture for each condition tested. *, statistically different from CTRL. (E, inset) Western blot analysis of endogenous PDK2 protein in Panc-1 cells in the absence or presence of siRNA-PDK2. (F) Real-time qPCR analysis of relative Bnip3Δex3 and Bnip3FL mRNA expression levels in Panc-1 cells. Cells were treated with 1–5 mM DCA. Data were obtained from at least $n = 3$ independent experiments for each condition tested. *, statistically different from CTRL in the absence of DCA. (G) Real-time qPCR analysis of relative Bnip3Δex3 mRNA and Bnip3FL mRNA in Panc-1 cells treated with pyruvate. Panc-1 cells were treated with 5 mM DCA or followed by knockdown of PDK2 with siRNA directed against

splicing (McFate et al., 2008). For these studies, Panc-1 cells were cultured in the presence of pyruvate in glucose and serum-free DMEM. As shown in Fig. 1 G, in contrast to Panc-1 cells grown in DMEM alone, a dose-dependent increase in exon 3 splicing of Bnip3 mRNA was observed in cells supplemented with pyruvate. Importantly, however, Bnip3 mRNA splicing was suppressed by either DCA or knockdown of PDK2 with or without pyruvate supplementation. Collectively, these findings strongly suggest that the glycolytic metabolism and the resultant increased PDK2 activity in cancer cells influences Bnip3 mRNA splicing and Bnip3Δex3 synthesis.

Alternative splicing of Bnip3Δex3 on cell survival during hypoxia

Because cancer cells are inherently resistant to metabolic stress imposed during hypoxia (Gillies and Gatenby, 2007b), we reasoned that hypoxia may influence Bnip3 pre-mRNA splicing and cell viability. To test this possibility, we assessed expression of Bnip3 isoforms under normoxic and hypoxic conditions. As shown in Fig. 1 H, in contrast to normoxic cells, a marked increase in both Bnip3FL and Bnip3Δex3 isoforms was detected in cardiac cells during hypoxia, a finding concordant with our previous work (Gang et al., 2011). Interestingly, however, Bnip3Δex3 isoform was highly expressed under normoxic conditions in Panc-1, HCT-116, and MCF-7 cells, and was further increased in each of the cancer cell lines tested during hypoxia (Fig. 1 H). Interestingly, while the Bnip3FL isoform was the dominant Bnip3 isoform detected in cardiac myocytes, the Bnip3Δex3 variant was the major Bnip3 isoform detected in each of the cancers during hypoxia.

As a step toward ascertaining whether the Bnip3Δex3 variant influences cell survival, we tested the impact of the Bnip3Δex3 isoform on cell viability during hypoxia. For these studies, cells were stained with vital dyes calcein-AM and ethidium homodimer-1 to identify the number of living (green) and dead (red) cells, respectively. As shown by epifluorescence microscopy in Fig. 1 (I and J), in contrast to cardiac myocytes, Panc-1, HCT-116, and MCF-7 cells were resistant to hypoxia. Based on the resistance of Panc-1, HCT-116, and MCF-7 cells to hypoxic injury, we reasoned that the high expression levels of Bnip3Δex3 spliced isoform in these cancer cells may confer a survival advantage during hypoxia. To test this possibility, we assessed whether selective knockdown of Bnip3Δex3 isoform would sensitize cancer cells to Bnip3FL and provoke cell death during hypoxia. For these studies, we generated siRNA directed against the unique exon 2–exon 4 junction sequences found exclusively in the Bnip3Δex3 isoform (Fig. 2 A). Previous work by our laboratory verified the specificity of the siRNA used for inhibiting the endogenous Bnip3Δex3 isoform in cardiac myocytes (Gang et al., 2011). As shown in Fig. 2 B, in contrast to normoxic control cells, Bnip3FL isoform expression was markedly increased in Panc-1 cells subjected to hypoxia. Importantly, neither Bnip3FL mRNA (Fig. 2 B) nor protein expression (Fig. 2 C) were affected by siRNA directed against Bnip3Δex3 isoform during hypoxia. These findings are in complete agreement with our previous work in cardiac myocytes demonstrating that siRNA used to knock down Bnip3Δex3 isoform in cancer cells does not influence the Bnip3FL mRNA or protein expression (Gang et al., 2011). In contrast, however, expression of endogenous Bnip3Δex3 isoform was dramatically reduced in cells expressing siRNA directed against Bnip3Δex3 isoform during hypoxia (Fig. 2, D and E). Notably, selective knockdown of endogenous Bnip3Δex3 isoform in Panc-1, HCT-116, and MCF-7 cells during hypoxia rapidly induced ROS production and cell death (Fig. 2, F–H; and Fig. S2, A–C). To further prove that cancer cells' resistance to Bnip3FL and hypoxia-induced cell death was dependent on the presence of Bnip3Δex3 isoform, we performed reciprocal experiments in which we selectively knocked down the Bnip3FL isoform but not Bnip3Δex3 spliced variant during hypoxia. For these studies, we generated shRNA directed against exon 3 sequences that are present in the Bnip3FL isoform but absent in the Bnip3Δex3 variant (Fig. 3 A). Notably, in contrast to control cells subjected to hypoxia, hypoxia-induced activation of endogenous Bnip3FL was markedly reduced by shRNA directed against the Bnip3FL isoform. Importantly, shRNA directed against Bnip3FL isoform had no effect on Bnip3Δex3 splicing during hypoxia (Fig. 2 C and Fig. 3, B and C). Furthermore selective knockdown of Bnip3FL isoform in Panc-1 and HCT-116 cells had no effect on hypoxia-induced cell death (Fig. 3, D and E). Collectively these findings strongly suggest that Bnip3FL provokes cell death in the absence of Bnip3Δex3 isoform. To validate these findings and the notion that the Bnip3Δex3 isoform confers a cell survival advantage in cancer cells by antagonizing the otherwise lethal effects of Bnip3FL isoform, we performed loss-of-function studies in which we knocked down Bnip3Δex3 variant in cancer cells overexpressing Bnip3FL. As shown in Fig. 4, knockdown of Bnip3Δex3 isoform sensitized Panc-1, HCT-116, and MCF-7 to cell death induced by Bnip3FL, a finding concordant with our cell viability data during hypoxia. Earlier work by our laboratory demonstrated that overexpression of Bnip3FL triggered mitochondrial perturbations and cell death of cardiac myocytes that was suppressed by Bnip3Δex3 isoform. Interestingly, as shown in Fig. 4 (A and B), Panc-1, HCT-116, and MCF-7 cells overexpressing the Bnip3FL isoform were indistinguishable from vector-transfected controls with respect to cell viability. However, knockdown for Bnip3Δex3 in cells overexpressing Bnip3FL unmasked the cytotoxic actions of Bnip3FL, triggering mitochondrial ROS production and cell death (Fig. 4, A–C). These important findings support our contention that in the absence of the Bnip3Δex3 spliced variant, the Bnip3FL isoform is cytotoxic to cells and provokes death. Collectively, these findings strongly suggest that the Bnip3Δex3 confers a survival advantage to cancer cells by antagonizing the lethal actions of Bnip3FL.

PDK2 in the absence or presence of 0.1–2 mM pyruvate. Data were obtained from at least $n = 3–4$ independent cell cultures for each condition tested. *, statistically different from CTRL; NS, not statistically different from each other in the indicated group; **, statistically different from CTRL in the absence of pyruvate. (H) Real-time PCR analysis of Bnip3FL and Bnip3Δex3 isoforms in NCMC, Panc-1, HCT116, and MCF-7 cells subjected to hypoxia (HPX) for 18 h. Data were obtained from at least $n = 3–4$ independent experiments for each condition tested. *, statistically different from myocytes CTRL for Bnip3FL isoform; †, not statistically different from myocytes CTRL for Bnip3FL isoform; **, statistically different from myocytes CTRL for Bnip3Δex3 isoform. (I) Cell viability of cancer cells during hypoxia; shown are representative epifluorescence images of cells stained with vital dyes calcein-AM and ethidium homodimer-1 to visualize live (green) and dead (red) cells, respectively, as we described previously. Bar, 40 µm. (J) Histogram depicting quantitative data from I. Data were obtained from at least $n = 3–4$ independent experiments counting ≥500 cells from $n = 3$ glass coverslips for each condition tested. *, statistically different from myocytes CTRL.

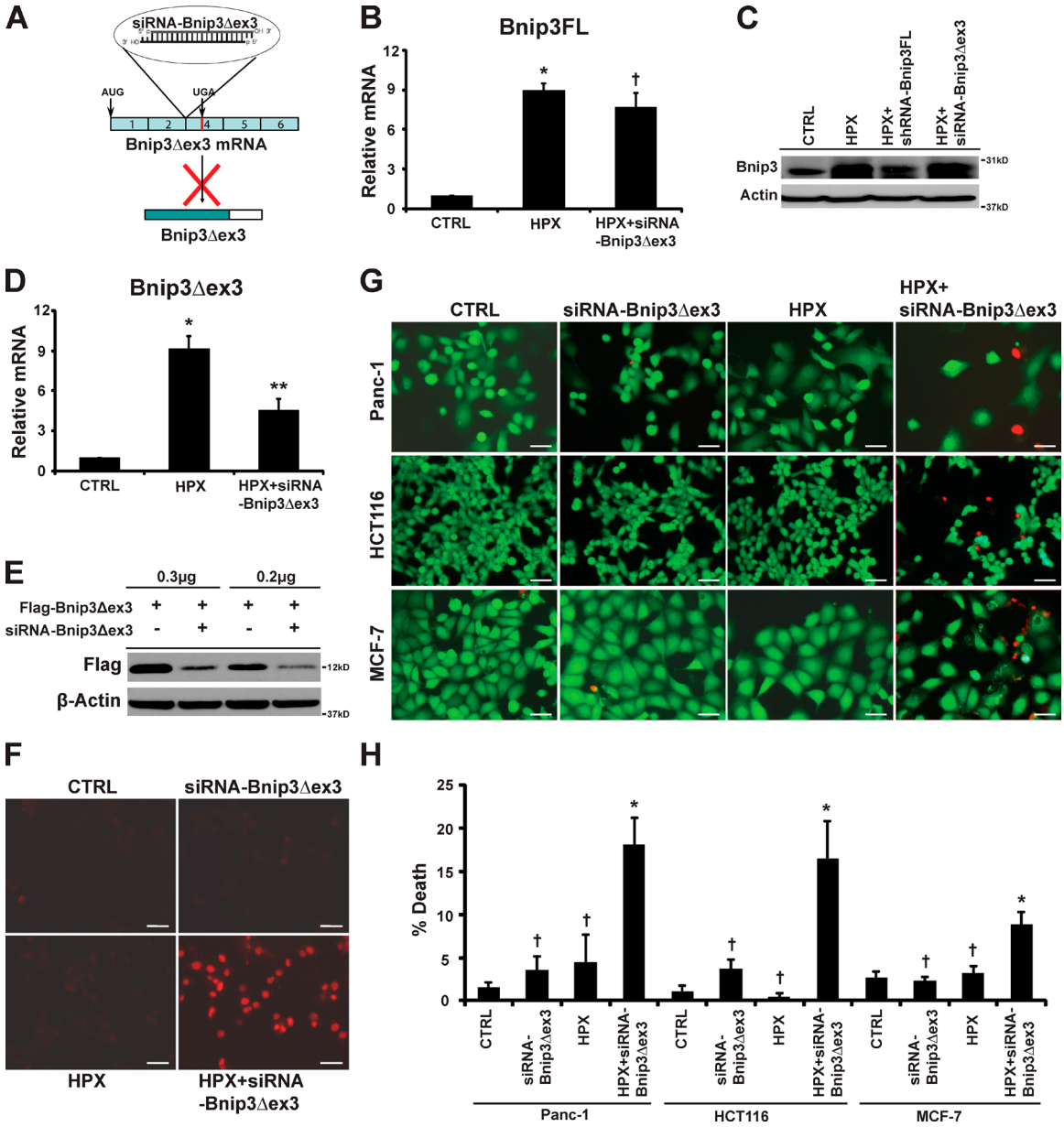

Figure 2. **Knockdown of Bnip3Δex3 isoform sensitizes cancer cells to hypoxia.** (A) Schematic depicting the targeting strategy of siRNA for knockdown of endogenous Bnip3Δex3 isoform. siRNA was designed to specifically target sequences spanning the exon 2–exon 4 junction, which is unique to the Bnip3Δex3 isoform. Specificity of the siRNA was described previously. (B) Real-time qPCR analysis of relative mRNA levels of endogenous Bnip3FL isoform. Panc-1 cells were subjected to hypoxia for 18 h in the absence or presence of siRNA-Bnip3Δex3 (50 nM). RNA extracted from the cells was analyzed by real-time PCR. Data were obtained from at least n = 3–4 independent experiments for each condition tested. Data are expressed as mean ± SD (error bars). *, statistically different from control (CTRL); †, not statistically different from HPX. (C) Western blot analysis of Bnip3 proteins in panc-1 cells in the absence or presence of shRNA-Bnip3FL or siRNA-Bnip3Δex3 under the hypoxia condition; the filter was probed with a murine antibody directed against Bnip3 (~30 kD). β-Actin (~40 kD) served as a loading control for the Western blot. (D) Real-time qPCR analysis of relative mRNA levels of endogenous Bnip3Δex3 isoform. Panc-1 cells were subjected to hypoxia for 18 h in the absence or presence of siRNA-Bnip3Δex3 (50 nM). RNA extracted from the cells was analyzed by real-time PCR. Data were obtained from at least n = 3–4 independent experiments for each condition tested. *, statistically different from control (CTRL); **, statistically different from hypoxia (HPX). (E) Western blot analysis of Flag-Bnip3Δex3 expression levels in Panc-1 cells. Panc-1 cells were transfected with Flag-Bnip3Δex3 eukaryotic expression vector in the absence or presence of siRNA-Bnip3Δex3. Bnip3Δex3 was detected with the antibody directed against Flag-tag. (F) ROS in Panc1 cells after Bnip3Δex3 knockdown during hypoxia; ROS production was monitored by dihydroethidium (DHE, red fluorescence) staining. Bars, 40 μm. (G) Cell viability of Panc-1, HCT116, and MCF-7 cells after Bnip3Δex3 knockdown during hypoxia. Cell viability was shown by representative epifluorescence images of cells stained with vital dyes calcein-AM and ethidium homodimer-1 to visualize live (green) and dead (red) cells, respectively. Bars, 40 μm. (H) Histogram for quantitative data shown in E. Data were obtained from at least n = 3–4 independent experiments counting ≥500 cells from n = 3 glass coverslips for each condition tested. *, statistically different from CTRL; †, not statistically different from CTRL.

Inhibition of Bnip3Δex3 promotes doxorubicin-induced cell death of cancer cells

Because earlier work by our laboratory established that the widely used chemotherapeutic agent doxorubicin promotes cardiac cell death by a mechanism contingent upon Bnip3FL (Dhingra et al., 2014), we reasoned that the preferential synthesis of Bnip3Δex3 isoform in cancer cells may antagonize Bnip3FL and

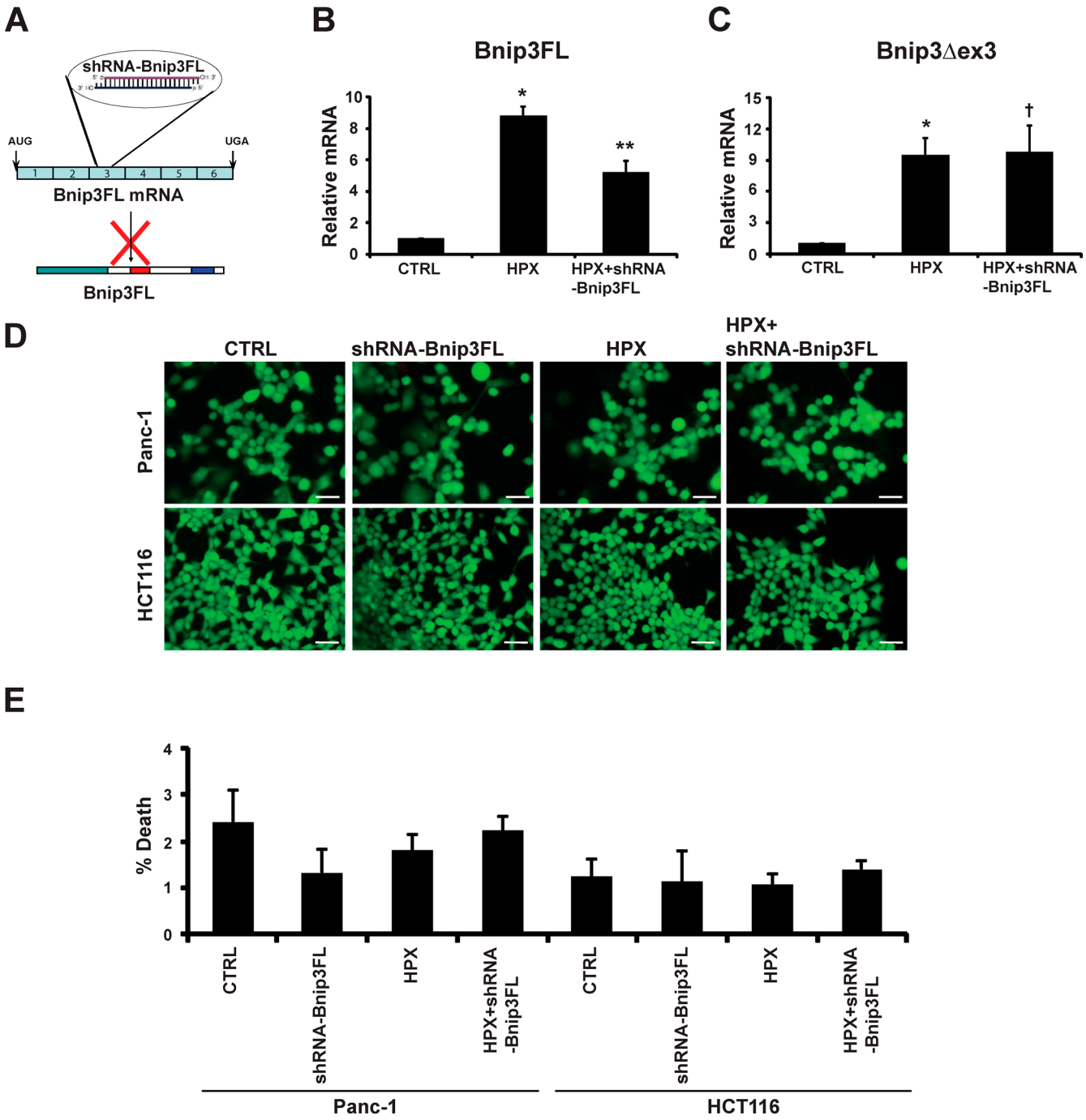

Figure 3. **Resistance of cancer cells to Bnip3FL isoform and hypoxia-induced cell death.** (A) Schematic depicting the targeting strategy of shRNA for knockdown of endogenous Bnip3FL. shRNA was designed to specifically target sequences within exon 3 of Bnip3FL to knock down Bnip3FL without interfering with Bnip3Δex3, as we have previously reported (Gang et al., 2011). (B and C) Real-time qPCR analysis of Bnip3FL (B) and Bnip3Δex3 (C) mRNA levels in cancer cells. Cells were subjected to hypoxia condition for 18 h in the absence or presence of shRNA-Bnip3FL. Data are expressed as mean ± SD (error bars). *, statistically different from control (CTRL); **, statistically different from HPX; †, not statistically different from HPX. Data were obtained from at least $n = 3–4$ independent cell cultures for each condition tested. (D) Cell viability of cancer cells after Bnip3FL knockdown with shRNA-Bnip3FL under hypoxic conditions. Shown are representative epifluorescence images of cells stained with vital dyes calcein-AM and ethidium homodimer-1 to visualize live (green) and dead (red) cells, respectively. Bars, 40 µm. (E) Histogram for quantitative data shown in E. Data were obtained from at least $n = 3–4$ independent cell cultures counting ≥500 cells from $n = 3$ glass coverslips for each condition tested.

underlie the reported resistance of cancers to doxorubicin treatment. Interestingly, a marked reduction in BrdU incorporation, Ki67 staining, and cell growth were observed in Panc-1 cells treated with doxorubicin, a finding concordant with the growth inhibitory effects of doxorubicin (Fig. 5, A–D). However, we observed no change in viability in either Panc-1 or HCT-116 cells treated with doxorubicin (Fig. 6, A and B). We speculated that the resistance of cancer cells to doxorubicin may be related to the relatively high endogenous levels of the Bnip3Δex3 in these cells. To test this possibility, we compared in parallel ex-

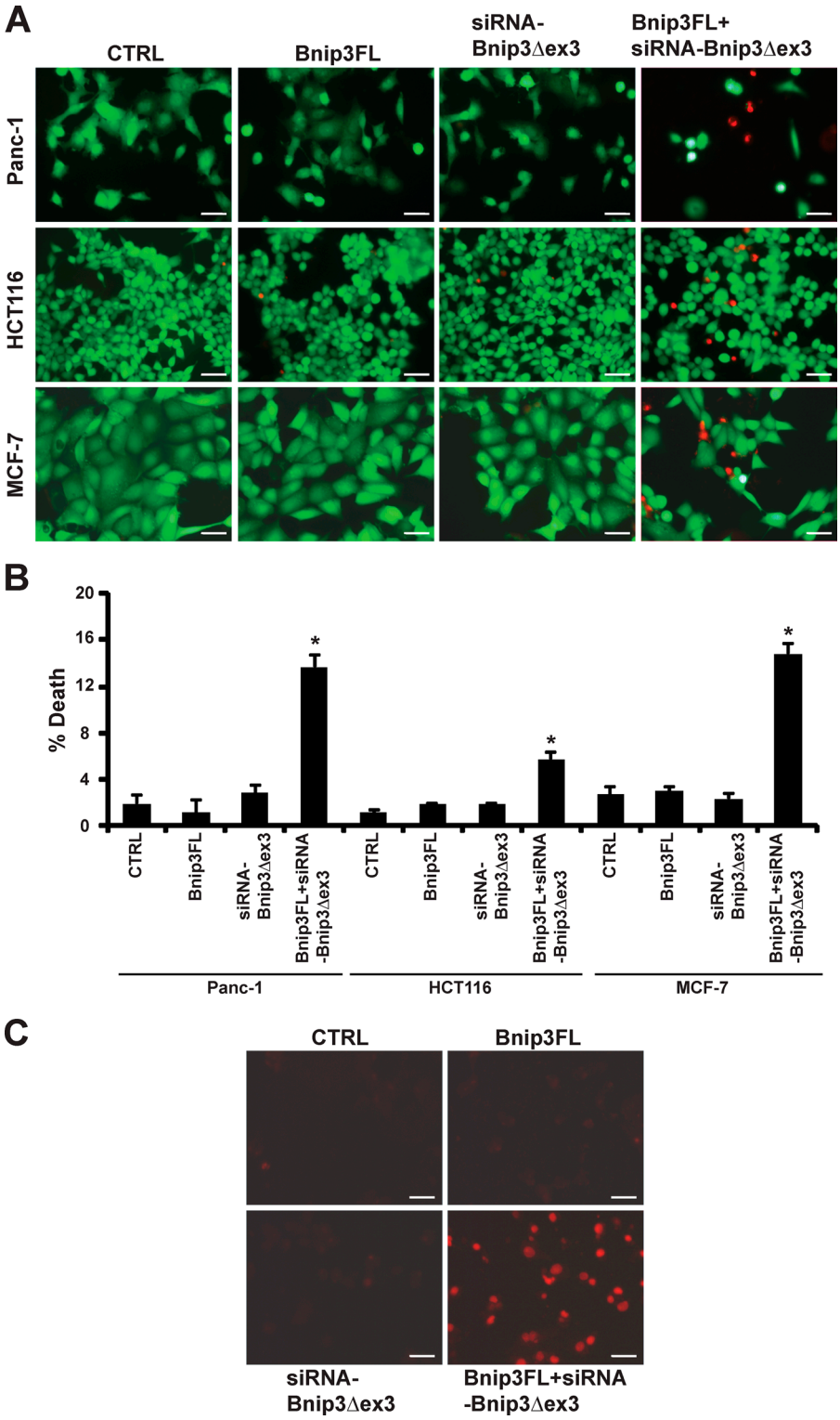

Figure 4. **Knockdown of Bnip3Δex3 sensitizes cancer cells to Bnip3FL-induced cell death.** (A) Cell viability of cancer cells expressing Bnip3FL in the absence and presence of siRNA-Bnip3Δex3. Representative epifluorescence images of various cancer cells stained with vital dyes calcein-AM and ethidium homodimer-1 to visualize live (green) and dead (red) cells, respectively. Bars, 40 µm. (B) Histogram for quantitative data shown in A. Data were obtained from at least n = 3–4 independent cell cultures counting ≥500 cells from n = 3 glass coverslips for each condition tested. *, statistically different from control (CTRL). (C) ROS production in Panc-1 cells (red fluorescence) overexpressing Bnip3FL in the absence and presence of Bnip3Δex3 knockdown with siRNA-Bnip3Δex3. Bars, 40 µm.

periments cell viability of Panc-1 and HCT-116 cancer lines to cardiac cells that express low basal levels of Bnip3Δex3 isoform to a wide dose range of doxorubicin. As shown in Fig. 6 (A and B), a marked dose-dependent increase in cardiac cell death was observed after doxorubicin treatment. This finding is in complete agreement with our earlier work demonstrating that cardiac myocytes are sensitive to doxorubicin (Dhingra et al., 2014). In contrast, however, Panc-1 and HCT-116 cancer cells were resistant to doxorubicin-induced cell death (Fig. 6, A and B).

Notably, knockdown of the Bnip3Δex3 isoform sensitized cancer cells to doxorubicin toxicity indicated by increased ROS production and cell death (Fig. 6, C–E). In converse experiments, knockdown of Bnip3FL isoform completely abrogated doxorubicin-mediated cell death in Panc-1 and HCT-116 cells (Fig. 6, F and G). These findings strongly suggest that Bnip3Δex3 isoform in cancer cells confers a survival advantage against doxorubicin-mediated cell death. Collectively, the data strongly support our contention that the preferential synthesis

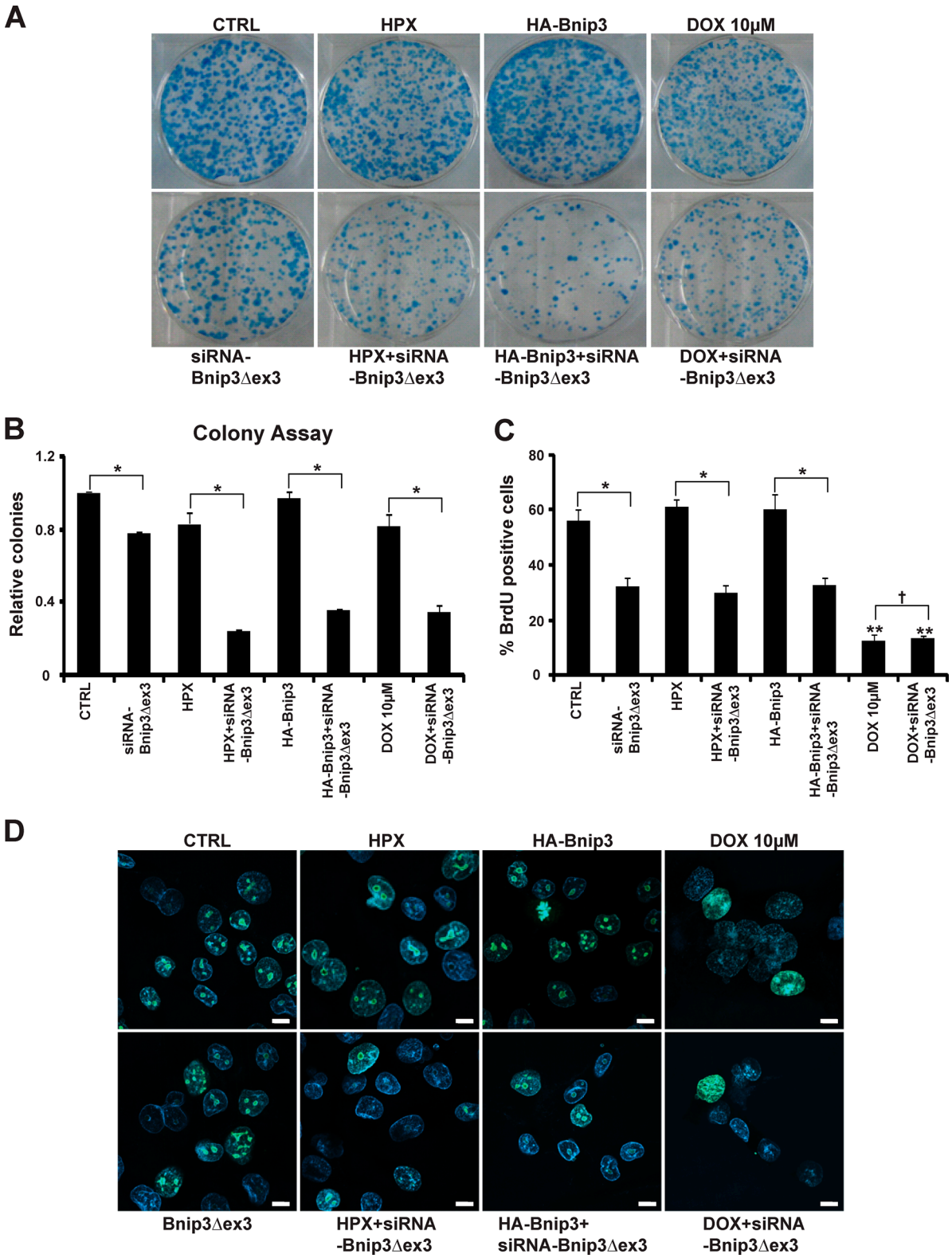

Figure 5. **Colony formation assay, BrdU incorporation, and Ki67 staining in HCT-116 and Panc-1 cancer cells.** (A) Colony formation assay in HCT116 cells in the absence and presence of siRNA directed against Bnip3Δex3 isoform subjected to hypoxia, transfected with HA-Bnip3, or treated with doxorubicin (10 μM DOX), respectively. (B) Histogram represents quantitative data for A. Data were obtained from at least $n = 3–4$ independent experiments for each condition tested. Data are expressed as mean ± SD (error bars). *, statistically different from each other. (C) Quantitative data for BrdU incorporation in Panc-1 cells in the absence and presence of siRNA directed against Bnip3Δex3 isoform subjected to hypoxia, transfected with HA-Bnip3, or treated with doxorubicin (10 μM DOX), respectively. Data were obtained from three independent cell cultures for each condition tested. *, statistically different from each other; **, statistically different from CTRL; †, not statistically different from each other. (D) Epifluorescence microscopy of Panc-1 cells stained for Ki67 protein (green) and Hoechst 33258 nuclear dye (blue). Cells were subjected to hypoxia, transfected with HA-Bnip3, or treated with doxorubicin (10 μM DOX) in the absence and presence of siRNA directed against Bnip3Δex3 isoform. Bars, 10 μm.

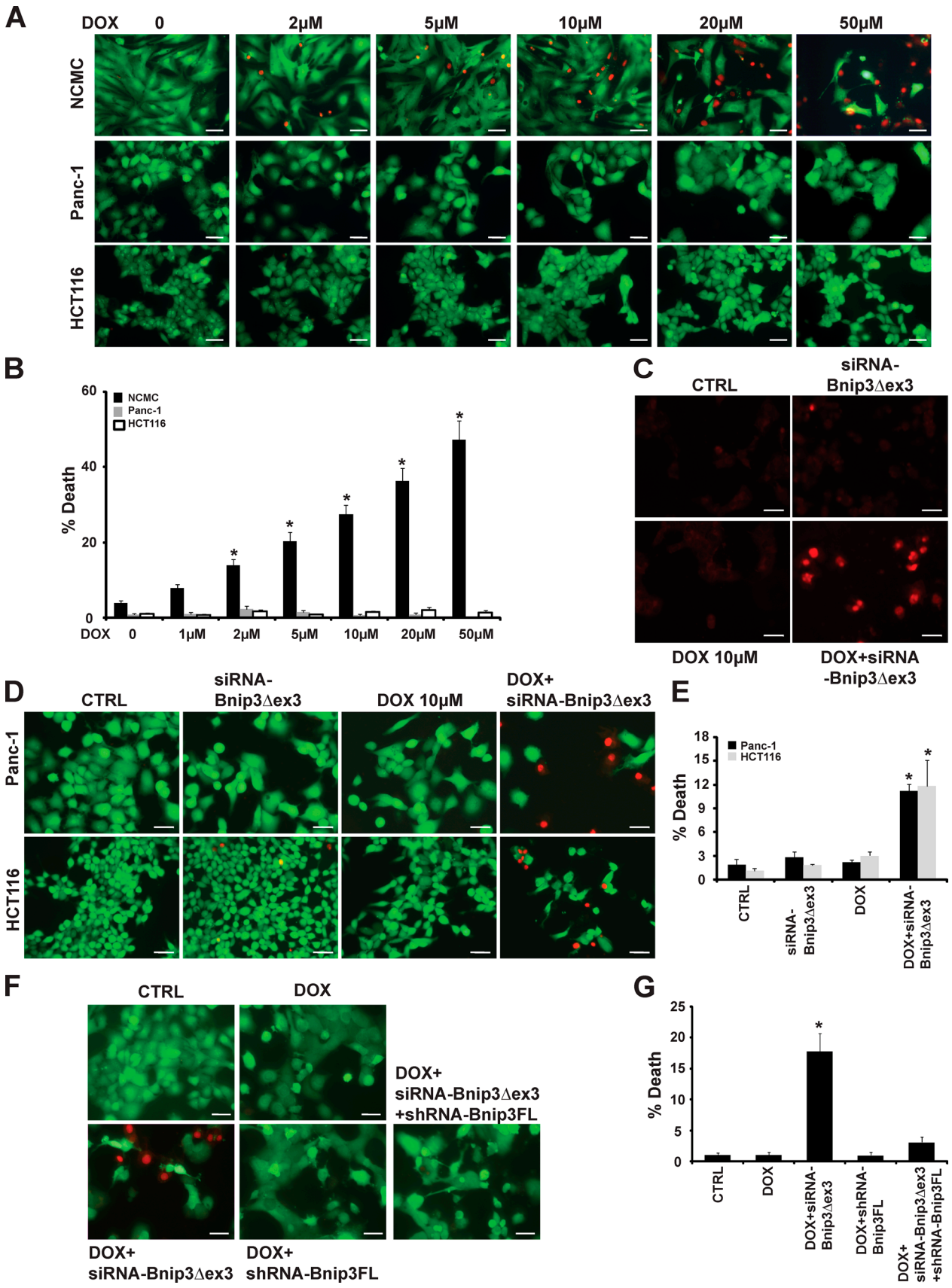

Figure 6. **Knockdown of Bnip3Δex3 promotes cell death induced by doxorubicin**. (A) Cell viability of neonatal cardiac myocytes (NCMC), Panc-1, and HCT116 cells treated with different concentrations of doxorubicin for 18 h. Representative epifluorescence images of cells stained with vital dyes calcein AM and ethidium homodimer-1 to visualize live (green) and dead (red) cells, respectively, are shown. Bars, 40 μm. (B) Histogram for quantitative data

of Bnip3Δex3 isoform in cancer cells confers a survival advantage against doxorubicin.

Bnip3FL is required for DCA-induced death of cancer cells

It was previously demonstrated that inhibition of PDK with DCA sensitized certain cancer cell to apoptosis (Bonnet et al., 2007). Because DCA suppressed alternative Bnip3 mRNA splicing and synthesis of Bnip3Δex3 survival isoform (Fig. 1 F), we reasoned that the cell death observed in cancer cells treated with DCA may be related to the unopposed actions of the Bnip3FL isoform. To test this possibility, we assessed the effects of DCA on cell viability in Panc-1 cells. As shown in Fig. 7 (A and B), a dose-dependent increase in cell death was observed in Panc-1 cells treated with DCA. Notably, this was accompanied by an increase in ROS production (Fig. 7 C). Interestingly, mitochondrial ROS production induced by DCA was completely abrogated by knockdown of Bnip3FL isoform. Notably, overexpression the Bnip3Δex3 isoform or knockdown of Bnip3FL abrogated cell death induced by DCA (Fig. 7, A–E). Further, the dependency of Bnip3 FL for the underlying cytotoxic effects of DCA was not restricted to Panc-1 cells, since similar observations were observed in HCT-116 and MCF-7 cells treated with DCA (Fig. S2, A–C). These findings substantiate that in the absence of Bnip3Δex3 isoform synthesis, DCA provokes cell death in cancer cells by a mechanism contingent upon Bnip3FL isoform.

Bnip3Δex3 promotes survival in cancer cells by suppressing mitochondrial targeting of Bnip3FL

Because our earlier work showed that interaction of the Bnip3Δex3 with Bnip3FL suppressed integration of Bnip3FL into mitochondrial membranes, as a central mechanism by which Bnip3Δex3 abrogates cell death induced by Bnip3FL, we tested whether the ability of the Bnip3Δex3 variant to suppress cell death in cancer cells was related to altered mitochondrial targeting of Bnip3FL. As shown by Western blot analysis in Fig. 8 A, Bnip3FL was predominately localized to the cytosolic fraction in Panc-1 cells under normoxic conditions. However, selective knockdown of endogenous Bnip3Δex3 isoform in cells subjected to hypoxia increased mitochondrial-associated Bnip3FL coincident with increased ROS production and cell death (Fig. 8, A–D), a finding concordant with our previous work in cardiac myocytes (Gang et al., 2011). Moreover, knockdown of Bnip3FL isoform in Panc-1, HCT-116, and MCF-7 cells that were also rendered deficient for Bnip3Δex3 isoform abrogated hypoxia-induced ROS production and cell death (Fig. 8, B–D; and Fig. S2, A–C). These findings verify that Bnip3FL promotes mitochondrial injury and cell death in the absence of Bnip3Δex3 isoform. Collectively, these findings strongly support the notion that Bnip3Δex3 variant suppresses cell death in cancer cells by interfering with the cytotoxic actions of Bnip3FL.

Discussion

In this report, we provide compelling new evidence that alternative gene splicing of Bnip3 pre-mRNA provides a molecular switch that determines whether Bnip3 triggers cell survival or death. We specifically show that in contrast to normal cells, the Bnip3Δex3 spliced variant that promotes survival is constitutively expressed and is the dominant Bnip3 mRNA isoform in cancer cells. Bnip3 is uniquely distinguished from other Bcl-2 proteins for several important and salient reasons. First, the Bnip3 promoter is transcriptionally silenced under basal normoxic conditions but is highly induced during hypoxia and ischemic stress. Second, Bnip3 can trigger perturbations to mitochondria consistent with permeability transition pore opening, loss of $\Delta\Psi m$, and ROS production (Shaw et al., 2006). Notably, knockdown of Bnip3, mutations of Bnip3 defective for mitochondrial targeting, or germ-line deletion of Bnip3 were each sufficient to suppress mitochondrial injury and cell death induced during hypoxia (Dhingra et al., 2014). Collectively these findings strongly support the notion and role for Bnip3 as a pro-death factor. However, despite these findings, certain cancer cells are reportedly resistant to cell death induced by Bnip3. In fact, there are some reports purporting a survival role for Bnip3 through autophagy (Mazure and Pouysségur, 2009). The underlying mechanisms for these discordant and confounding observations are unknown. This raises the question of how Bnip3 can elicit such dramatic and varied effects on cell fate, on the one hand promoting survival while on the other promoting cell death. During the course of our investigations, we discovered a previously unrecognized Bnip3 transcript deleted for exon 3 (Bnip3Δex3) in normal cardiac cells in vitro and in vivo. Interestingly, the alternative spliced variant, Bnip3Δex3, was virtually undetectable in normal cells under basal normoxic conditions but was readily detected during ischemic or hypoxic stress. These findings indicated that not only was Bnip3 gene transcription induced in response to hypoxia but that hypoxic stress provides a signal for alterative gene splicing of Bnip3 mRNA. Moreover, while the Bnip3 protein encoded by the full-length Bnip3 mRNA Bnip3FL provoked mitochondrial perturbations and widespread cell death, the Bnip3 protein encoded by truncated spliced variant Bnip3Δex3 (deleted for exon 3) promoted cell survival. The significance of the Bnip3Δex3 isoform in tumor cells is unknown and had not been previously investigated. Considering that alternative gene splicing of metabolic, cell cycle, and growth-related genes are associated with tumori-

shown in A. Data were obtained from at least n = 3–4 independent experiments counting ≥500 cells from n = 3 glass coverslips for each condition tested. (C) ROS production by DHE staining in Panc-1 cells treated with DOX (10 µM) for 18 h in the absence or presence of Bnip3Δex3 knockdown with siRNA-Bnip3Δex3. Bars, 40 µm. (D) Cell viability of Panc-1 and HCT-116 cancer cells treated with doxorubicin (10 µM) for 18 h in the absence and presence of Bnip3Δex3 knockdown with siRNA-Bnip3Δex3. Representative epifluorescence images of cells stained with vital dyes calcein AM and ethidium homodimer-1 to visualize live (green) and dead (red) cells, respectively, are shown. Bars, 40 µm. (E) Histogram for quantitative data shown in D. Data were obtained from at least n = 3–4 independent experiments counting ≥500 cells from n = 3 glass coverslips for each condition tested. (F) Cell viability of cancer cells treated with doxorubicin (10 µM) for 18 h in the absence or presence of siRNA-Bnip3Δex3 and shRNA-Bnip3FL, respectively. Representative epifluorescence images of cells stained with vital dyes calcein AM and ethidium homodimer-1 to visualize live (green) and dead (red) cells, respectively, are shown. Bars, 40 µm. (G) Histogram for quantitative data shown in F. Data were obtained from at least n = 3–4 independent experiments counting ≥500 cells from n = 3 glass coverslips for each condition tested. Data are expressed as mean ± SD (error bars). *, statistically different from control (CTRL).

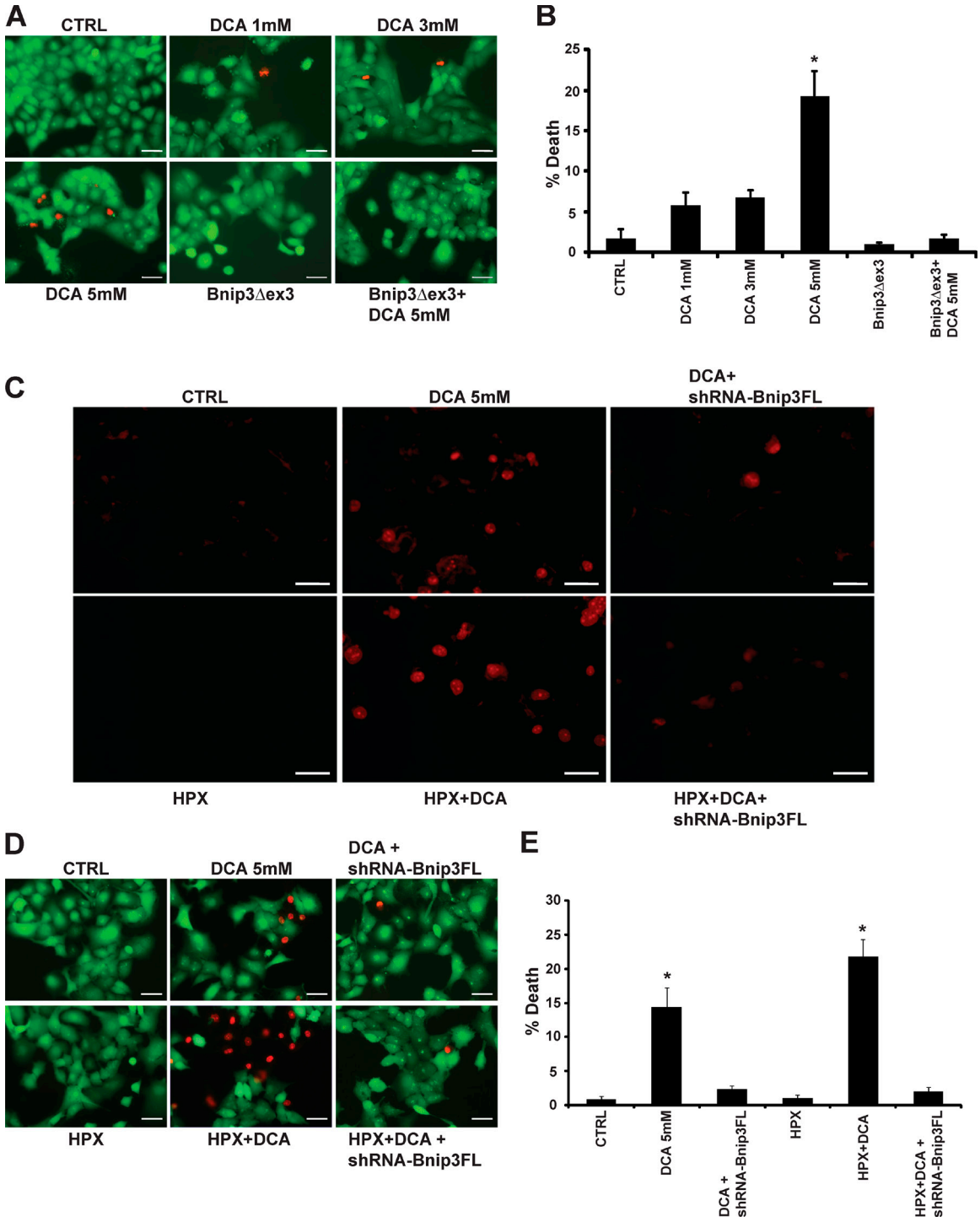

Figure 7. **Selective knockdown of Bnip3FL rescues cell death induced by DCA.** (A) Cell viability of Panc-1 cells expressing Bnip3Δex3 in the absence or presence of 1–5 mM DCA for 24 h. Representative epifluorescence images of cells stained with vital dyes calcein AM and ethidium homodimer-1 to visualize live (green) and dead (red) cells, respectively, are shown. Bars, 40 µm. (B) Histogram for quantitative data shown in A. Data were obtained from at least n = 3–4 independent experiments counting ≥500 cells from n = 3 glass coverslips for each condition tested. (C–E) ROS (C) and cell viability (D and E) of Panc-1 cells treated with 5 mM DCA for 24 h in the absence or presence of shRNA-Bnip3FL during hypoxia. Representative epifluorescence images of cells stained with vital dyes calcein AM and ethidium homodimer to visualize live (green) and dead (red) cells, respectively, are shown. ROS production was monitored by DHE staining. Bars, 40 µm. (E) Histogram for quantitative data shown in D. Data were obtained from at least n = 3–4 independent experiments counting ≥500 cells from n = 3 glass coverslips for each condition tested. Data are expressed as mean ± SD (error bars). *, statistically different from CTRL.

genesis, it would be reasonable to consider that preferential synthesis of the survival isoform of Bnip3Δex3 generated by alternative splicing would confer a growth advantage and adaptive resistance of tumor cells to hypoxia. Herein, we provide novel evidence that the Bnip3 mRNA spliced variant Bnip3Δex3, which promotes cell survival, is preferen-

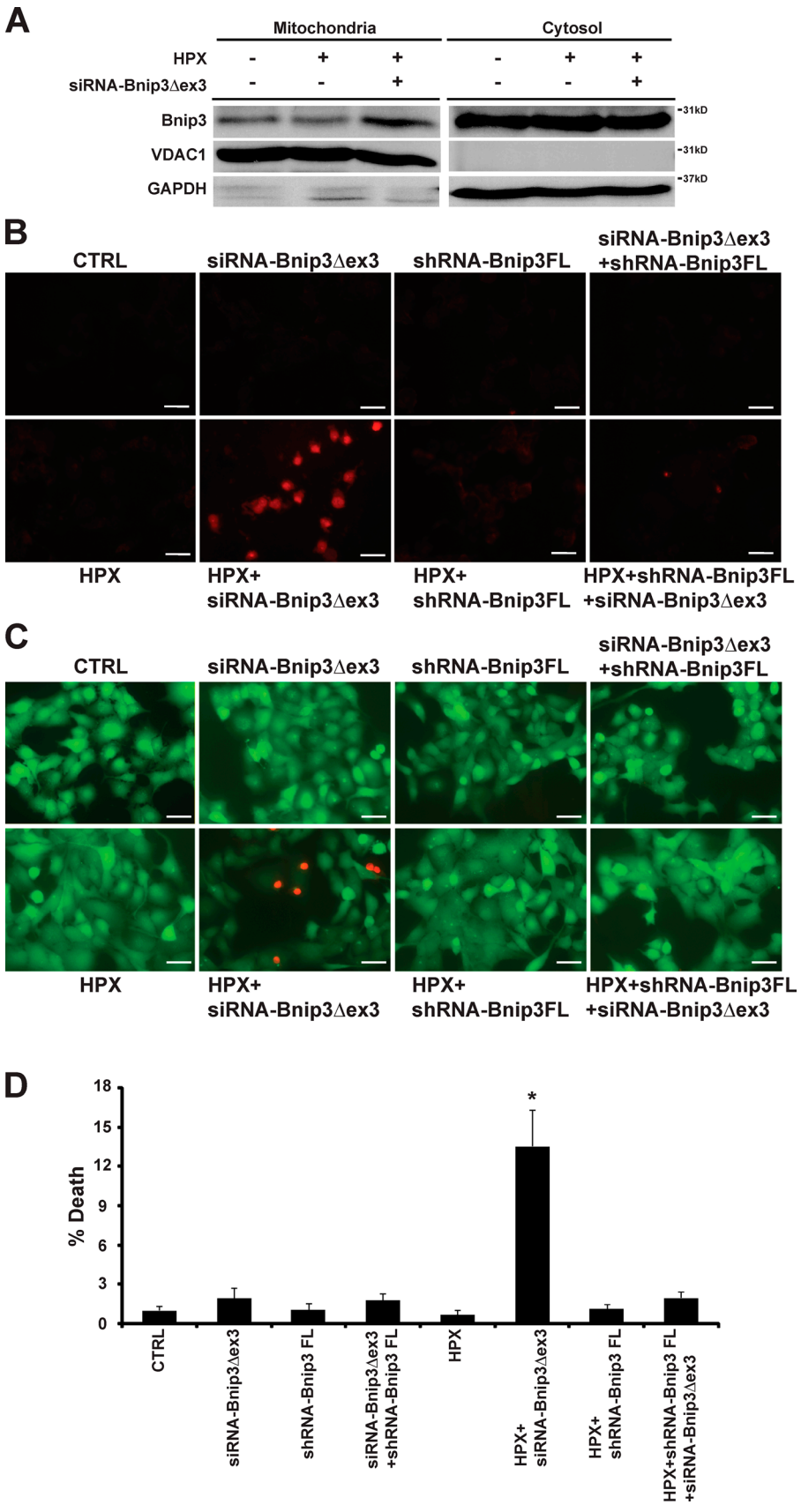

Figure 8. **Mitochondrial targeting of Bnip3FL isoform in Panc-1 is increased in Panc-1 cells deficient for Bnip3Δex3 variant.** (A) Mitochondrial targeting of Bnip3FL is increased in Panc-1 cells during hypoxia after knockdown of Bnip3Δex3 isoform. Western blot analysis of mitochondrial and cytoplasmic fractions under normoxic and hypoxic conditions in the absence and presence of Bnip3Δex3 knockdown is shown; the filter was probed with a murine antibody directed against mitochondrial protein VDAC1, or cytosolic protein GAPDH was used to verify the integrity and purity of the cell fractionation. Bnip3FL was detected with a murine antibody directed against Bnip3. (B) ROS production in panc-1 cells after Bnip3Δex3 knockdown with siRNA-Bnip3Δex3 under hypoxia conditions. Epifluorescence microscopy of Panc-1 cells monitored for ROS production by DHE (red fluorescence). Bars, 40 µm. (C) Cell viability. Representative epifluorescence images of cells stained with vital dyes calcein-AM and ethidium homodimer-1 to visualize live (green) and dead (red) cells for conditions shown in B are shown. Bars, 40 µm. (D) Histogram for quantitative data shown in C. Data were obtained from at least n = 3–4 independent experiments counting ≥500 cells from n = 3 glass coverslips for each condition tested. Data are expressed as mean ± SD (error bars). *, statistically different from control (CTRL).

tially synthesized as the primary Bnip3 transcript in cancer cells. This is coincident with the resistance of these cells to hypoxic injury. Indeed, even under basal conditions, the Bnip3Δex3 isoform was highly expressed in several different cancers and tumor cell lines studied. That Bnip3Δex3 may provide a growth advantage to cancer cells is substantiated by

the unexpected decrease in cell proliferation in Panc-1 cells after Bnip3Δex3 knockdown. This raises the possibility that in addition to cell survival, Bnip3Δex3 may also play a role in cell growth. However, further studies are required to address this property of Bnip3Δex3.

While the mechanisms that underlie alternative splicing of Bnip3 pre-mRNA in tumor cells were not studied here and were not an active area of investigation in our laboratory, we believe the elevated and preferential synthesis of the Bnip3Δex3 isoform over Bnip3FL likely reflects an intrinsic survival mechanism linked to metabolic remodeling that protects tumor cells against mitochondrial injury and that would otherwise occur during hypoxic tumorigenesis (Gatenby et al., 2007). The fact that splicing of Bnip3Δex3 was inhibited and cell death was increased by DCA treatment is compelling and strongly supports our contention that the preferential synthesis of survival Bnip3Δex3 isoform in cancer cells is linked to the glycolytic phenotype and PDK2 for apoptosis resistance (Verduzco et al., 2015; Wojtkowiak et al., 2015). This view is further substantiated by the fact that cell death induced by DCA was completely abrogated in cells after inhibition of Bnip3FL, supporting our contention that in the absence of Bnip3Δex3 spliced isoform, Bnip3FL is cytotoxic to cells and promotes cell death. Indeed, we showed by not one but by three independent approaches that inhibition of PDK2, which inhibited Bnip3Δex3 mRNA splicing, decreased the ratio of Bnip3Δex3/Bnip3FL and sensitized cancer cells to Bnip3FL and hypoxia-induced cell death. Hence, the resistance of certain cancer cells to hypoxia or chemotherapeutic agents may be related to the presence of Bnip3Δex3 and the ratio to the Bnip3FL isoform. Indeed, selective inhibition of the Bnip3Δex3 isoform in each of the cancer cell lines studied provoked widespread death in response to Bnip3FL or doxorubicin. Interestingly, while cell proliferation and cell growth were inhibited in Panc-1 cells treated with doxorubicin, cell death induced by doxorubicin was not increased in these cells unless Bnip3Δex3 isoform was inhibited. These findings strongly suggest that preferential synthesis of Bnip3Δex3 isoform in cancer cells confers a survival advantage by opposing the lethal actions of the Bnip3FL isoform.

That mitochondrial-associated Bnip3FL was dramatically increased in the absence of Bnip3Δex3 isoform strongly suggests that Bnip3Δex3 likely interferes with Bnip3FL's ability to provoke mitochondrial perturbations and cell death. This view is consistent with increased cell death induced by Bnip3FL in cells deficient for Bnip3Δex3 subjected to hypoxia. Together, our data strongly suggest that Bnip3Δex3 variant, at least operationally, promotes tumor cell survival during hypoxia by curtailing mitochondrial injury and activation of cell death pathways induced by Bnip3FL.

A recent study by Mazure and Pouysségur (2009) purported a survival role for Bnip3 through autophagy. This was based on an apparent increased cell death of MCF-7 cells after knockdown of Bnip3. However, the siRNA used to silence Bnip3FL in that study was targeted against sequences within exon 4. Because exon 4 is also present in Bnip3Δex3 survival isoform, we believe that the reported increased cell death was due to the inhibition of the survival isoform Bnip3Δex3, which predisposed cells to death and led Mazure and Pouysségur (2009) to inadvertently conclude that there was a survival role for Bnip3FL. This view is supported by our present findings in which cell death and not autophagy was dramatically increased in MCF-7 cells after inhibition of Bnip3Δex3 survival isoform. Further, the fact that knockdown of Bnip3Δex3 sensitized cancer cells to hypoxia and doxorubicin-induced cell death supports our contention that the Bnip3FL isoform in the absence of Bnip3Δex3 spliced variant promotes cell death and not survival. We believe the Bnip3Δex3 isoform confers a survival advantage by dampening or curtailing mitochondrial injury triggered by Bnip3FL in a cell- and context-specific manner. In fact, in the absence of Bnip3Δex3 isoform, Bnip3FL triggered maladaptive autophagy and necrotic cell death (unpublished data). Therefore, we believe the alternative spliced isoform of Bnip3Δex3 promotes cell survival by antagonizing the otherwise lethal actions of Bnip3FL isoform. Therefore, we believe that the discordant and confounding reports on Bnip3′s ability to provoke cell death may be explained by the following: first, the unappreciated existence of the Bnip3Δex3 spliced variant, which promotes survival; second, the majority of studies concluding a role for Bnip3 in survival and/or autophagy were conducted in cell lines with high basal levels of the endogenous Bnip3Δex3 survival isoform, which would have blocked cell death induced by Bnip3FL.

Another interesting and important aspect the present study was the detection of Bnip3Δex3 variant in several different human breast and glioblastoma tumors. The significance of this finding, however, is presently unknown. As we currently do not know whether the expression of Bnip3Δex3 isoform correlated with the stage or invasiveness of the tumor, it will therefore be important to assess this aspect of the Bnip3Δex3 isoform in future studies. Based on the findings of the present study, we would predict that tumors expressing high basal levels of survival isoform of Bnip3Δex3 would exhibit resistance to hypoxia and chemotherapy. Given the findings of the present study as well as others (Gustafsson, 2011), we speculate that Bnip3FL may be important for regulating mitochondrial quality control by targeting removal of mitochondria during cellular stress that would promote glucose oxidation by glycolysis. Because unopposed actions of Bnip3FL would otherwise promote excessive mitochondrial loss during tumorigenesis, we believe that generation of the Bnip3Δex3 isoform would allow cancer cells to modulate Bnip3FL levels and fine tune mitochondrial numbers commensurate with the cell's energy requirements for growth and proliferation. This view is consistent with the concept of mitochondrial culling by Nix for reticulocyte maturation (Novak et al., 2010; Bhandari et al., 2014).

To our knowledge, our data provide the first direct evidence for the existence of a novel survival isoform of Bnip3 generated by alternative gene splicing in cancer cells. We further demonstrate that the alternative splicing of Bnip3 is linked to PDK2 and the unique glycolytic phenotype in cancer cells. We further show that expression of Bnip3FL isoform in the absence of Bnip3Δex3 spliced variant is cytotoxic and promotes widespread death of several different human cancer cells. Hence, our findings may not only explain the discordant and confounding reports regarding Bnip3′s effects on cell fate but fundamentally explain how the glycolytic metabolism in cancer cells overrides cell death during hypoxia tumorigenesis. Therapeutic agents designed to selectively inhibit Bnip3Δex3 isoform may prove beneficial in modulating cell death induced by Bnip3FL and tumor development during hypoxia.

Materials and methods

Cell culture and transfection

Pancreatic ductal carcinoma (Panc-1), human colon carcinoma (HCT116), and human Caucasian breast adenocarcinoma (MCF-7) cells were grown in DMEM 10% FBS as reported. Cells were treated with doxorubicin (DOX, 10 µM; Pfizer) or DCA (1–5 mM; Sigma-Aldrich) for up to 18 h (Dhingra et al., 2014). Cells were transfected with 0.2 µg plasmids of Bnip3FL or Bnip3Δex3 with an Effectene transfection kit (QIAGEN; Gang et al., 2011). Postnatal ventricular myocytes were isolated from 1–2-d-old Sprague-Dawley rats and cultured under serum-free DMEM/F12 medium as described previously. Cells were subjected to hypoxia for up to 24 h in an air-tight chamber under serum-free culture conditions continually gassed with 95% N_2-5% CO_2, $pO_2 \leq 2$–5 mmHg, as we reported previously (Regula et al., 2002; Gang et al., 2011).

Quantitative real time PCR

Total RNA from cells was extracted with GenElute mammalian total RNA miniprep kit from Sigma-Aldrich. Then 1 µg of total RNA was reverse transcribed with oligo dT_{20} (Invitrogen), and one twentieth of the reaction was amplified with gene-specific primers for Bnip3, Bnip3Δex3, or housekeeping control gene L32, respectively. Real-time RT-PCR was performed using iQ5 multicolor Real-time PCR detection system (Bio-Rad Laboratories; Gang et al., 2011).

Cloning and constructs

The Bnip3 gene was amplified from rat genomic DNA while Bnip3Δex3 PCR product was purified from radioactive gel. Both PCR products were cloned into pcDNA3-HA expression vector or pcDNA3-Flag vector (CMV promotor and pcDNA backbone; Invitrogen) to generate expression plasmids encoded either Bnip3 or Bnip3Δex3 HA-tag or Flag-tag constructs. ShRNA-Bnip3FL was designed to specifically target exon 3 of full-length Bnip3 (Bnip3FL), and the sequence was 5′-CACCGACACCACAAGATACCAAC AGCGAACTGTTGGTATCTTGTGGTGTC-3′. shRNA-Bnip3FL was constructed with BLOCK-iT U6 RNAi entry vector kit (Invitrogen) and the control LacZ shRNA was provided in the kit. The sequence was 5′-CACCGCTACACAAATCAGCGATTTCGAA AAATCGCTGATTTGTGTAG-3′. siRNA-Bnip3Δex3 to knock down Bnip3 spliced variant (Bnip3Δex3) was designed to target the exon 2–4 junction and the sequence was 5′-CACTGTGACAGTC TGAGGATT-3′ (Gang et al., 2011); the scramble control siRNA sequence was 5′-CACCGCTACACAAATCAGCGATT-3′. The siRNA-PDK2 oligo was purchased from Invitrogen (5′-GCCTGCCT GTCTACAACAA-3′); the negative siRNA control sequence is 5′-GCCGTCCATCTAACGTCAA-3′. All the constructs were confirmed by DNA sequencing.

Cell viability

Cell viability was determined using the vital dyes calcein-acetoxymethyl ester (2 µM) to determine the number of living cells (green fluorescence) and ethidium homodimer-1 (2 µM) to determine the number of dead cells (red fluorescence; Molecular Probes), as we previously reported. Cells were visualized with a research fluorescence microscope (AX-70; Olympus) under the magnification of 200× at room temperature in DMEM/F12 serum-free medium. Image acquisition was accomplished by Image-Pro plus 5.0 software. Cells were analyzed from at least $n = 3$–4 independent cultures counting ≥300 cells for each condition tested. Data are expressed as the mean ± SE percentage from control (Gang et al., 2011; Dhingra et al., 2014).

ROS

Cells were visualized using a research-grade epifluorescence microscope (AX-70; Olympus). To monitor ROS production, cells were incubated with 2.5 µM dihydroethidium (Molecular Probes) at 37°C for 30 min (Dhingra et al., 2014).

Western blot analysis and ELISA

Cell lysates (20 µg) were resolved on a 4–20% SDS-PAGE gel. Bnip3 proteins were detected using a monoclonal murine antibody raised against amino acid residues 1–163 of human Bnip3 (Ray et al., 2000). Cytoplasmic and mitochondrial fractions of cell lysate were prepared as previously reported (Regula et al., 2002). Murine antibodies directed toward GAPDH (1 µg/ml; Sigma-Aldrich) or VDAC 1 (1 µg/ml; Cell Signaling Technology) were used to verify the integrity of the preparation. Bound proteins were visualized using enhanced chemiluminescence reagents ECL (Pharmacia, Inc.). The PDK2 kinase activity was determined by ELISA using the phospho S293 PDH E1 α protein ELISA kit (Abcam). Cells were collected with NP-40 lysis buffer and 20 µg of the protein was used for the assay as per the manufacturer's instructions.

Colony proliferation assay

Cells were plated as single cell suspension at very low density (1,000 cells in 2 ml medium on a 35-mm dish) for 7–9 d, after which cells were fixed in methanol containing 1% methylene blue in the absence and presence of interventions as detailed in the figure legends.

BrdU incorporation and Ki67 staining

The BrdU labeling and detection kit (Roche) was used to detect the BrdU incorporation into cellular DNA as per the manufacturer's instructions. Cells were fixed and visualized with a research fluorescence microscope (AX10 Observer SD; Carl Zeiss) at 200× magnification at room temperature. Ki67 protein was detected by immunostaining of Panc-1 cells using a rabbit antibody directed against Ki67 (1:50 dilution; Abcam) and secondary goat anti–rabbit conjugated Alexa Fluor 488 (1:200 dilution; Molecular Probe). Hoechst 33258 nuclear dye was used to visualize the nucleus. Cells were fixed and imaged with a research fluorescence microscope (AX10 Observer SD) under the magnification of 630× at room temperature. Image acquisition was performed using ZEN software (Carl Zeiss).

Radiolabeled RT-PCR for cells and breast tumors

Five tumors were randomly selected from the Manitoba Breast Tumor Bank, which operates with the approval of the Faculty of Medicine, University of Manitoba Research Ethics Board. Total RNA was extracted from frozen tissue sections using TRIzol reagent (GIBCO BRL; as described previously). For radioactive RT-PCR, total RNA from cells and tissue was reverse transcribed and amplified in 25 cycles with Bnip3 primers, with the reverse primer ^{32}P-labeled. The PCR products were resolved on 8% polyacrylamide/8 M Urea denaturing gels. The gel was dried, exposed, and scanned in a PhosphorImager (Fuji Medical Systems). All ^{32}P-labeled Bnip3 PCR products were verified by Sanger sequencing as we previously reported (Gang et al., 2011).

Statistical analysis

Multiple comparisons between groups were determined by analysis of variance (ANOVA). An unpaired two-tailed Students *t* test was used to compare mean differences between groups. Differences were considered to be statistically significant to a level of $P < 0.05$. In all cases the data were obtained from at least $n = 3$–4 independent cell cultures using $n = 3$ replicates for each condition tested unless stated otherwise in the figure legend.

Online supplemental material

Fig. S1 shows that Bnip3Δex3 is constitutively present in human cancers. Fig. S2 shows the effects of Bnip3Δex3 spliced variant on cell survival of HCT-116 and MCF-7 cancer cells. Online supplemental material is available at http://www.jcb.org/cgi/content/full/jcb.201504047/DC1.

Acknowledgments

We are grateful to the friendship of the late Dr. Arnold H. Greenberg. We thank Dr. H. Weisman for critical comments on the manuscript. We thank F. Aguilar and Nichol Garcia for technical assistance. We would like to thank Joe Garcia for helpful discussions on DCA.

This work was supported by grants to L.A. Kirshenbaum from the Canadian Institutes of Health Research (MOP42402, MOP244369, and MOP74456) and from the St. Boniface Hospital Research Foundation. L.A. Kirshenbaum holds a Canada Research Chair in Molecular Cardiology.

The authors declare no competing financial interests.

Submitted: 10 April 2015
Accepted: 7 August 2015

References

Ashwell, J.D., N.A. Berger, J.A. Cidlowski, D.P. Lane, and S.J. Korsmeyer. 1994. Coming to terms with death: apoptosis in cancer and immune development. *Immunol. Today.* 15:147–151. http://dx.doi.org/10.1016/0167-5699(94)90309-3

Bellot, G., R. Garcia-Medina, P. Gounon, J. Chiche, D. Roux, J. Pouysségur, and N.M. Mazure. 2009. Hypoxia-induced autophagy is mediated through hypoxia-inducible factor induction of BNIP3 and BNIP3L via their BH3 domains. *Mol. Cell. Biol.* 29:2570–2581. http://dx.doi.org/10.1128/MCB.00166-09

Bhandari, P., M. Song, Y. Chen, Y. Burelle, and G.W. Dorn II. 2014. Mitochondrial contagion induced by Parkin deficiency in *Drosophila* hearts and its containment by suppressing mitofusin. *Circ. Res.* 114:257–265. http://dx.doi.org/10.1161/CIRCRESAHA.114.302734

Bonnet, S., S.L. Archer, J. Allalunis-Turner, A. Haromy, C. Beaulieu, R. Thompson, C.T. Lee, G.D. Lopaschuk, L. Puttagunta, S. Bonnet, et al. 2007. A mitochondria-K+ channel axis is suppressed in cancer and its normalization promotes apoptosis and inhibits cancer growth. *Cancer Cell.* 11:37–51. http://dx.doi.org/10.1016/j.ccr.2006.10.020

Chiche, J., M. Rouleau, P. Gounon, M.C. Brahimi-Horn, J. Pouysségur, and N.M. Mazure. 2010. Hypoxic enlarged mitochondria protect cancer cells from apoptotic stimuli. *J. Cell. Physiol.* 222:648–657.

Christofk, H.R., M.G. Vander Heiden, M.H. Harris, A. Ramanathan, R.E. Gerszten, R. Wei, M.D. Fleming, S.L. Schreiber, and L.C. Cantley. 2008. The M2 splice isoform of pyruvate kinase is important for cancer metabolism and tumour growth. *Nature.* 452:230–233. http://dx.doi.org/10.1038/nature06734

Dhingra, R., V. Margulets, S.R. Chowdhury, J. Thliveris, D. Jassal, P. Fernyhough, G.W. Dorn II, and L.A. Kirshenbaum. 2014. Bnip3 mediates doxorubicin-induced cardiac myocyte necrosis and mortality through changes in mitochondrial signaling. *Proc. Natl. Acad. Sci. USA.* 111:E5537–E5544. http://dx.doi.org/10.1073/pnas.1414665111

Gang, H., Y. Hai, R. Dhingra, J.W. Gordon, N. Yurkova, Y. Aviv, H. Li, F. Aguilar, A. Marshall, E. Leygue, and L.A. Kirshenbaum. 2011. A novel hypoxia-inducible spliced variant of mitochondrial death gene Bnip3 promotes survival of ventricular myocytes. *Circ. Res.* 108:1084–1092. http://dx.doi.org/10.1161/CIRCRESAHA.110.238709

Gang, B.P., P.J. Dilda, P.J. Hogg, and A.C. Blackburn. 2014. Targeting of two aspects of metabolism in breast cancer treatment. *Cancer Biol. Ther.* 15:1533–1541. http://dx.doi.org/10.4161/15384047.2014.955992

Garon, E.B., H.R. Christofk, W. Hosmer, C.D. Britten, A. Bahng, M.J. Crabtree, C.S. Hong, N. Kamranpour, S. Pitts, F. Kabbinavar, et al. 2014. Dichloroacetate should be considered with platinum-based chemotherapy in hypoxic tumors rather than as a single agent in advanced non-small cell lung cancer. *J. Cancer Res. Clin. Oncol.* 140:443–452. http://dx.doi.org/10.1007/s00432-014-1583-9

Gatenby, R.A., and R.J. Gillies. 2007. Glycolysis in cancer: a potential target for therapy. *Int. J. Biochem. Cell Biol.* 39:1358–1366. http://dx.doi.org/10.1016/j.biocel.2007.03.021

Gatenby, R.A., K. Smallbone, P.K. Maini, F. Rose, J. Averill, R.B. Nagle, L. Worrall, and R.J. Gillies. 2007. Cellular adaptations to hypoxia and acidosis during somatic evolution of breast cancer. *Br. J. Cancer.* 97:646–653. http://dx.doi.org/10.1038/sj.bjc.6603922

Gillies, R.J., and R.A. Gatenby. 2007a. Adaptive landscapes and emergent phenotypes: why do cancers have high glycolysis? *J. Bioenerg. Biomembr.* 39:251–257. http://dx.doi.org/10.1007/s10863-007-9085-y

Gillies, R.J., and R.A. Gatenby. 2007b. Hypoxia and adaptive landscapes in the evolution of carcinogenesis. *Cancer Metastasis Rev.* 26:311–317. http://dx.doi.org/10.1007/s10555-007-9065-z

Gustafsson, A.B. 2011. Bnip3 as a dual regulator of mitochondrial turnover and cell death in the myocardium. *Pediatr. Cardiol.* 32:267–274. http://dx.doi.org/10.1007/s00246-010-9876-5

Hamacher-Brady, A., N.R. Brady, R.A. Gottlieb, and A.B. Gustafsson. 2006. Autophagy as a protective response to Bnip3-mediated apoptotic signaling in the heart. *Autophagy.* 2:307–309. http://dx.doi.org/10.4161/auto.2947

Israelsen, W.J., T.L. Dayton, S.M. Davidson, B.P. Fiske, A.M. Hosios, G. Bellinger, J. Li, Y. Yu, M. Sasaki, J.W. Horner, et al. 2013. PKM2 isoform-specific deletion reveals a differential requirement for pyruvate kinase in tumor cells. *Cell.* 155:397–409. http://dx.doi.org/10.1016/j.cell.2013.09.025

Mazure, N.M., and J. Pouysségur. 2009. Atypical BH3-domains of BNIP3 and BNIP3L lead to autophagy in hypoxia. *Autophagy.* 5:868–869. http://dx.doi.org/10.4161/auto.9042

McFate, T., A. Mohyeldin, H. Lu, J. Thakar, J. Henriques, N.D. Halim, H. Wu, M.J. Schell, T.M. Tsang, O. Teahan, et al. 2008. Pyruvate dehydrogenase complex activity controls metabolic and malignant phenotype in cancer cells. *J. Biol. Chem.* 283:22700–22708. http://dx.doi.org/10.1074/jbc.M801765200

Novak, I., V. Kirkin, D.G. McEwan, J. Zhang, P. Wild, A. Rozenknop, V. Rogov, F. Löhr, D. Popovic, A. Occhipinti, et al. 2010. Nix is a selective autophagy receptor for mitochondrial clearance. *EMBO Rep.* 11:45–51. http://dx.doi.org/10.1038/embor.2009.256

Plas, D.R., and C.B. Thompson. 2002. Cell metabolism in the regulation of programmed cell death. *Trends Endocrinol. Metab.* 13:75–78. http://dx.doi.org/10.1016/S1043-2760(01)00528-8

Ray, R., G. Chen, C. Vande Velde, J. Cizeau, J.H. Park, J.C. Reed, R.D. Gietz, and A.H. Greenberg. 2000. BNIP3 heterodimerizes with Bcl-2/Bcl-X(L) and induces cell death independent of a Bcl-2 homology 3 (BH3) domain at both mitochondrial and nonmitochondrial sites. *J. Biol. Chem.* 275:1439–1448. http://dx.doi.org/10.1074/jbc.275.2.1439

Regula, K.M., K. Ens, and L.A. Kirshenbaum. 2002. Inducible expression of BNIP3 provokes mitochondrial defects and hypoxia-mediated cell death of ventricular myocytes. *Circ. Res.* 91:226–231. http://dx.doi.org/10.1161/01.RES.0000029232.42227.16

Robey, I.F., R.M. Stephen, K.S. Brown, B.K. Baggett, R.A. Gatenby, and R.J. Gillies. 2008. Regulation of the Warburg effect in early-passage breast cancer cells. *Neoplasia.* 10:745–756. http://dx.doi.org/10.1593/neo.07724

Shaw, J., T. Zhang, M. Rzeszutek, N. Yurkova, D. Baetz, J.R. Davie, and L.A. Kirshenbaum. 2006. Transcriptional silencing of the death gene BNIP3 by cooperative action of NF-κB and histone deacetylase 1 in ventricular myocytes. *Circ. Res.* 99:1347–1354. http://dx.doi.org/10.1161/01.RES.0000251744.06138.50

Verduzco, D., M. Lloyd, L. Xu, A. Ibrahim-Hashim, Y. Balagurunathan, R.A. Gatenby, and R.J. Gillies. 2015. Intermittent hypoxia selects for genotypes and phenotypes that increase survival, invasion, and therapy resistance. *PLoS ONE.* 10:e0120958.

Wang, E.Y., H. Gang, Y. Aviv, R. Dhingra, V. Margulets, and L.A. Kirshenbaum. 2013. p53 mediates autophagy and cell death by a mechanism contingent on Bnip3. *Hypertension.* 62:70–77. http://dx.doi.org/10.1161/HYPERTENSIONAHA.113.01028

Warburg, O. 1956. On the origin of cancer cells. *Science.* 123:309–314. http://dx.doi.org/10.1126/science.123.3191.309

Wojtkowiak, J.W., H.C. Cornnell, S. Matsumoto, K. Saito, Y. Takakusagi, P. Dutta, M. Kim, X. Zhang, R. Leos, K.M. Bailey, et al. 2015. Pyruvate sensitizes pancreatic tumors to hypoxia-activated prodrug TH-302. *Cancer Metab.* 3:2. http://dx.doi.org/10.1186/s40170-014-0026-z